J Comp Physiol A (2011) 197:1173–1187
DOI 10.1007/s00359-011-0679-9

ORIGINAL PAPER

Visual response properties of neck motor neurons in the honeybee

Y.-S. Hung · J. P. van Kleef · M. R. Ibbotson

Received: 31 May 2011 / Revised: 26 August 2011 / Accepted: 28 August 2011 / Published online: 11 September 2011

Abstract Recent behavioural studies have demonstrated that honeybees use visual feedback to stabilize their gaze. However, little is known about the neural circuits that perform the visual motor computations that underlie this ability. We investigated the motor neurons that innervate two neck muscles (m44 and m51), which produce stabilizing yaw movements of the head. Intracellular recordings were made from five (out of eight) identified neuron types in the first cervical nerve (IK1) of honeybees. Two motor neurons that innervate muscle 51 were found to be direction-selective, with a preference for horizontal image motion from the contralateral to the ipsilateral side of the head. Three neurons that innervate muscle 44 were tuned to detect motion in the opposite direction (from ipsilateral to contralateral). These cells were binocularly sensitive and responded optimally to frontal stimulation. By combining the directional tuning of the motor neurons in an opponent manner, the neck motor system would be able to mediate reflexive optomotor head turns in the direction of image motion, thus stabilising the retinal image. When the dorsal ocelli were covered, the spontaneous activity of neck motor neurons increased and visual responses were modified, suggesting an ocellar input in addition to that from the compound eyes.

Y.-S. Hung · J. P. van Kleef · M. R. Ibbotson
ARC Centre of Excellence in Vision Science,
Research School of Biology and Division of Biomedical Science and Biochemistry, R.N. Robertson Building, Australian National University, Canberra, ACT 2601, Australia

Y.-S. Hung · M. R. Ibbotson (✉)
National Vision Research Institute,
Australian College of Optometry, Corner Keppel and Cardigan Streets, Carlton, VIC 3053, Australia
e-mail: mibbotson@nvri.org.au

Keywords Direction selective · Temporal tuning · *Apis mellifera* · Head movement · Insect

Introduction

Insects move their heads relative to their bodies for many reasons, some reflexive and others generated from active 'decisions' (e.g. Land 1973; Hengstenberg 1984; Sobel 1990; Baader 1991; Gilbert et al. 1995). Head movements during free flight have an important role in separating the optic flow that occurs across the retina into rotational and translational components, thus mediating good spatial vision during complex locomotion (Kern et al. 2005; Karmeier et al. 2006; Lindeman et al. 2008). This is achieved using a mode of flight in which the animals shift their gaze direction actively using saccade-like movements of the head, followed by a turning movement of the body in the same direction. Immediately after the saccade-like turns, there is a period in which the animal flies essentially straight with its head stabilised to minimise rotational signals (flies: van Hateren and Schilstra 1999; honeybees: Böddeker and Hemmi 2010; Böddeker et al. 2010). While the image motion during the large saccade-like movements of the head is probably actively 'ignored' using some type of saccadic suppression mechanism (Ibbotson et al. 2008), it is essential to detect any unintended rotations of the head that occur during the straight flight segment (Böddeker et al. 2010). It is well established that such relatively low-speed rotations can be detected and compensated for using the optomotor head-turning reflex (Hengstenberg et al. 1986). As an example, if an insect's head unintentionally rotates to the left, image motion travels rightward across the retina. To reduce image blur the head is turned to the right to momentarily stabilise the retinal image, as is the

case for ocular following in primates (e.g. Ibbotson et al. 2007). Between the saccadic head movements, the angular head velocities of flies are reduced to values of 0–100°/s, which is low enough to limit visual blur and maintain a fixed head gaze direction (van Hateren and Schilstra 1999).

To drive head movements it is necessary for the nervous system to detect the direction of wide-field image motion and transfer the signal to the motor neurons that drive appropriate head and body movements. Considerable effort has gone into recording the response properties of direction-selective neurons in insect brains (e.g. fly: Hausen 1982; Krapp and Hengstenberg 1996; Wertz et al. 2009ab; honeybee: Ibbotson and Goodman 1990; Ibbotson 1991). However, with a few notable exceptions in the fly (e.g. Milde et al. 1987; Strausfeld et al. 1987; Gilbert et al. 1995; Huston and Krapp 2008; 2009) and bee (Schröter et al. 2007), there has been relatively little recording of visual responses from the motor neurons that form the final neural output in the neck region. The response properties and connectivity of the motor neurons are interesting because they form the link between the motion signals calculated in the optic lobes and optomotor behaviour. Recordings made from fly neck motor neurons suggest that some behave much like direction-selective neurons in the optic lobes when the eyes are stimulated with wide-field moving patterns (Milde et al. 1987), although binocular interactions become more prominent (Huston and Krapp 2008). It was also noted that many fly motor neurons were multi-sensory, responding to mechanical stimulation of the wings and antennae (Milde et al. 1987) or to simultaneous stimulation of the mechanosensory halteres and the visual motion pathway (Huston and Krapp 2009).

In honeybees, many muscles in the thorax are involved in head movements, potentially including those that superficially appear to move the forelegs (Snodgrass 1942; Markl 1966; Berry and Ibbotson 2010). The most obvious muscles that have involvement are muscles 40–44, which connect the thorax and head and are known as direct muscles. Six other muscles (45–51) connect between different parts of the prothorax and deform the exoskeleton in the neck region. These six muscles have a central role in assisting head turns in various planes (Berry and Ibbotson 2010). The neck muscles are controlled via three paired nerves, IK1, IK2 and IN1. Schröter et al. (2007) traced the morphology of the eight motor neurons in the first cervical nerve, IK1, from their cell bodies in the suboesophageal ganglion (SOG) to their terminals in neck muscles 44 and 51, thus providing a baseline for physiological investigation at the single cell level. Muscle 44 is a large direct-muscle that connects the prothorax to the head capsule. Its connections suggest possible involvement in the control of head retraction, in head declination (nose-down pitch) and unilateral adduction (head yaw) control (Fig. 1a, b). Muscle 51 is an indirect-muscle that retracts the frontal exoskeleton of the prothorax. It is thought that the direct muscles pull the head firmly against the prothorax while indirect muscles, such as muscle 51, unilaterally retract the front of the prothorax, thus differentially changing the locations of the two horizontally aligned pivot points on which the head sits (the occipital processes: see Fig. 10 and associated text). The combination of these two effects is to give the head a substantial amount of freedom to move in the horizontal plane, as outlined in detail elsewhere (Berry and Ibbotson 2010). It is very likely that muscle 51 is, therefore, involved in controlling yawing movements of the head (Fig. 1b, c).

Figure 1c shows reconstructions of the eight motor neurons in the SOG (modified from Schröter et al. 2007). The dendrites of the neurons are all located in the dorso-lateral region of the SOG. While the study by Schröter and colleagues revealed the detailed anatomical connectivity of the motor neurons and showed extracellular evidence that they were visually active, it was not possible to match the identities of particular neurons to their physiological properties. This limits the interpretation of the directional properties of the cells in the context of the head movements that could be generated reflexively during image motion. That study was also limited to the investigation of visual inputs in general. The present work uses intracellular recording, with subsequent dye filling to assess the relative contributions from the compound and simple eyes (ocelli), revealing that both visual systems provide input. We show recordings from five of the identified neuron types in the first cervical nerve and find that they are visually sensitive and direction-selective. Their directional tuning matches the expected role in driving particular head movements. By conducting intracellular recordings in the present work, it was possible to measure not only spiking activity but also the membrane properties of the neurons. We found that profound changes in mean membrane potential occur even in the axons, suggesting an additional role for slow potentials in controlling head movements.

Materials and methods

Animals

Experiments were conducted on honeybees, *Apis mellifera*, that had been actively foraging. Hives were situated at the Australian National University. Each bee was lightly anaesthetized by cooling. The wings were then removed, and it was placed dorsal side down into an earthed metal holder. Recordings were made from nerve IK1, which exits the ventral nerve cord between the suboesophageal and prothoracic ganglia (Fig. 1a). The cervical region was exposed by tilting the head backwards by approximately 30°. It was

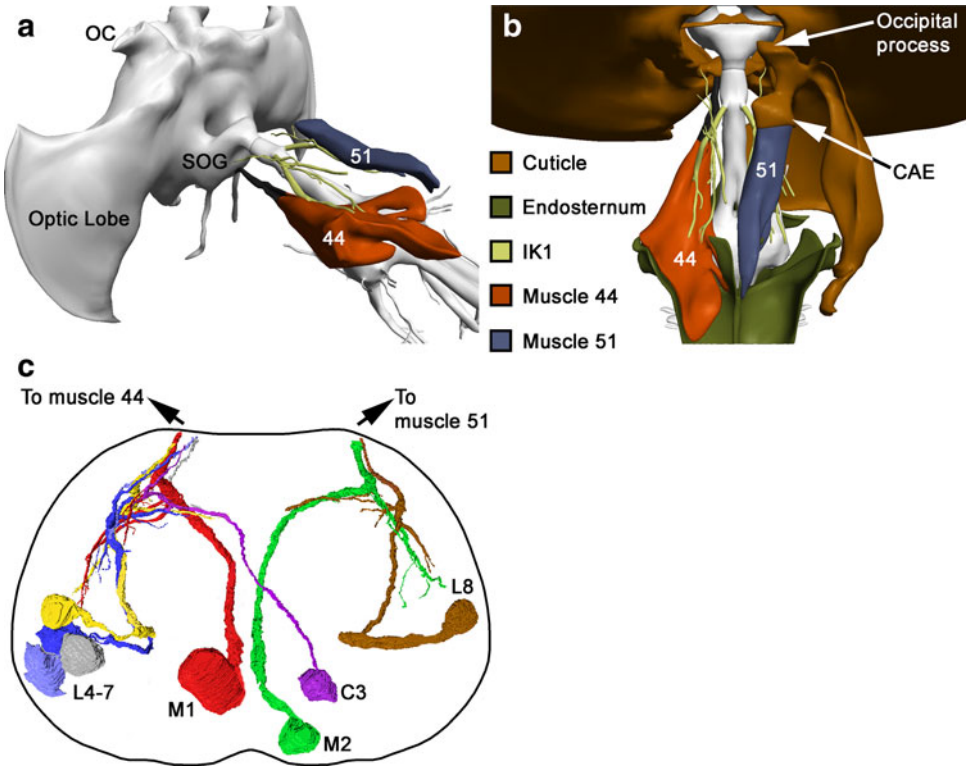

Fig. 1 Anatomy of the honeybee neck. **a** Birdseye view of the honeybee brain and ventral nerve cord from the rear left quarter (*grey tissue*). The ocelli (OC) and suboesophageal ganglion (SOG) are labelled. Nerve IK1 is shown in *yellow* and originates from the nerve cord close to the SOG. Muscle 51 is shown in *blue* and muscle 44 is shown in *orange*. **b** A dorsal view of the neck region showing the same structures as in **a** but also with the rear of the head capsule (*brown*), the right-hand exoskeleton of the prothorax (*brown*) and the endosternum (*green*) shown. Muscle 51 connects posteriorly with the endosternum and anteriorly with the cervical apodeme of the endosternum (CAE). When muscle 51 contracts it pulls the CAE inwards, thus also swinging the occipital process inwards (allowing the head to yaw). Muscle 44 connects extensively with the endosternum posteriorly and connects directly to the lower head capsule anteriorly. **c** Three-dimensional reconstructions of motor neurons in the SOG that travel through nerve IK1 (adapted from Schröter et al. 2007). The reconstructions show the main branches of the cells but not the fine dendrites. The *black outline* shows the outer limits of the SOG. Muscle 44 is innervated by six motor neurons (M1, C3 and L4-7). These are shown on the left side of the SOG. Muscle 51 is innervated by two motor neurons (M2 and L8), shown on the right of the SOG

then secured with sticky wax and the episternum, basisternum, fore-legs and neck membrane were removed.

Recording

Bees were inverted and placed in front of a stimulus monitor. The bees were allowed to recover from anaesthesia for at least 20 minutes before electrophysiology began. Recording electrodes were advanced into IK1 from the bee's underside. Intracellular recording and dye injection were performed using microelectrodes pulled from thin-walled filamentous capillary glass (o.d. 1.0 mm, i.d. 0.7 mm; Clark Electromedical GC100TF-10). The electrodes were filled with Lucifer Yellow (5% Lucifer Yellow CH in 0.2 M LiCl; Invitrogen, USA). Electrode tip resistances were approximately 150 MΩ. Chloride coated silver wires were used as the indifferent electrodes and positioned in the exposed thorax just posterior to the prothoracic ganglion. Cell penetration was aided by briefly increasing the feedback gain in the capacity compensation circuit of the amplifier. Recording periods in individual preparations did not usually exceed 20 min, which was the time required to run a subset of experiments, before iontophoretic injection of dye. We were able to obtain stable recordings and fills from 30 cells for the full 20 min.

Signals were amplified using a DC-amplifier (Getting Model 5A) and filtered (LP cut-off 1 kHz) and then acquired at 25 kHz with a 1401*plus* interface and Spike2 software (Cambridge Electronic Design, Cambridge, UK). The spikes were passed through a Schmitt trigger, producing TTL pulses at the time of each action potential. These pulses were used by Spike2 to generate online peri-stimulus time histograms (PSTHs) of the spiking activity. Offline, data was re-analysed in detail. Isolations were excellent with signal to noise ratios in excess of 10:1. No spike sorting algorithms were required to isolate particular spikes. All presented data are from single cell recordings.

The response frequency was calculated relative to the mean ongoing activity of the cell, which was measured in periods before and after each experimental test and subsequently averaged over periods of several minutes.

After isolating a neuron, handheld stimuli were moved around the bee's head to determine if visual responses were present and air was moved over the head by blowing through a straw. Neurons were tested for visual responses quantitatively using custom visual stimuli produced on two devices. Device 1 was a VSG Series 2/5 stimulus generator (Cambridge Research Systems, Cambridge, UK). Stimuli were presented on a gamma-corrected monitor running at 198 Hz (Clinton Monoray, 57 cd/m^2 mean luminance, 600 × 400 pixels) at a viewing distance of 8 cm. The monitor subtended 134 × 124° at the eye and could be moved such that it covered the frontal visual fields of both eyes (positioned perpendicular to the animals longitudinal axis), or to stimulate either the left or right eye (for arrangement details see Schröter et al. 2007). In the latter case, the screen was perpendicular to an axis inclined 45° to the antero-posterior axis of the head. Stimuli were high contrast (0.6) sine-wave gratings that could be moved back and forth at any angle on the screen. A range of spatial and temporal frequencies was used. The highest temporal frequency used was 48 Hz.

To measure the directional tuning properties of the cells we used moving sine wave gratings (spatial frequency: 0.02 cpd). As the spontaneous activities could fluctuate suddenly, directional and temporal frequency tuning functions were collected quickly. They were most often obtained by measuring the responses to grating movements during time intervals of 500 ms followed by 1 s rest periods. As 18 directions of image motion were tested, a complete directional tuning function could be achieved in 27 s and this sequence was repeated as often as possible (at least 3 times to produce a valid data set). For low temporal frequencies (<1 Hz), it was necessary to increase the stimulus duration to allow the grating to move a reasonable distance across the receptive field. For those experiments, the stimulus period was extended to 3 s, with a 3 s rest period.

Device 2 was a custom-built, wide-field stimulus consisting of a display with 9 columns of LEDs, each column containing 12 pairs of UV and green LEDs (Roithner Lasertechnik 380D15, peak emission at 383 nm; Roithner Lasertechnik B5-433-B525, peak emission at 528 nm). There were 216 LEDs arranged on the surface of a sphere of radius 120 mm. Each bee's head was positioned at the centre of the sphere by locating it at the point of intersection of two aligned laser pointers attached to the stimulus. From the bee's point of view, the intervals between LEDs in the vertical direction (elevation) were 6° and in the horizontal direction (azimuth) were 12°. The display subtended 96° in azimuth and 66° in elevation, sufficient to cover a large portion of most receptive fields. While the separation of LEDs was large, the stimuli were typically moved at high speeds and no evidence of aliasing was observed. The directional tuning obtained using device 2 was the same as that obtained using device 1.

The electronic control used the sample-and-hold concept described by Lindemann et al. (2003) and was described in detail previously (Berry et al. 2006). The refresh rate was 625 Hz. The usage of sample-and-hold circuitry allows all LEDs to be switched on continuously, with a maximum intensity of $\sim 10^{14}$ photons cm^{-2} s^{-1}. This is sufficient to obtain an overall brightness that matches an equivalent patch of daylight sky. We presented moving bars on the screen and at times presented full-field flashed stimuli.

Neuronal responses to individual stimulus presentations were aligned relative to a synchronisation pulse provided by the stimulus generation computer in the blanking interval prior to the first stimulus frame. Responses were measured as the mean number of spikes in the stimulus time window. The mean preferred direction of motion for each cell was obtained by calculating the mean vector angle of the circular histogram (Batschelet 1981; Ibbotson and Goodman 1990).

Staining and histology

Lucifer Yellow was injected into the neurons after recordings using a 3–6 nA hyperpolarizing DC-current. The dye was given 30 min diffusion time and then the brains were fixed (2.0 g paraformaldehyde, 17 ml 2.25% NaOH, 83 ml 2.555% $NaHzPO_4$, 2 ml 100 mM $CaC1_2$), dehydrated in an ethanol series, cleared (using methyl salicilate) and viewed on a Nikon Optiphot epifluorescence microscope. When the quality of the filled neuron was acceptable, the neuron was optically sectioned on either a BioRad LaserSharp2000 or a Leica SP2 UV confocal microscope (Fig. 2). To allow easy identification of the main features of the cells, without autofluorescence obscuring some of the fine details, we have provided black and white drawings of all cells. These were made in Photoshop by drawing over the photomicrographs produced by the confocal microscope.

Results

Intracellular recording from motor neurons in IK1 proved a difficult technical challenge. To maintain neural health it was necessary to leave the nerve connected to the muscles, which periodically contracted. The nerve was stabilised to some extent by suspending it over a metal wire that had been glued to the thorax but muscle contractions were still able to move the electrode out of the cell. Holding cells for

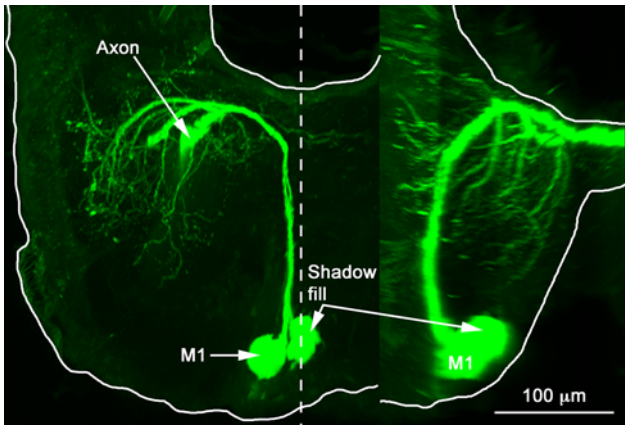

Fig. 2 Dye fill of motor neuron M1. On the left is a dorsal view of the suboesophageal ganglion (SOG). On the right is a lateral view. The recorded cell was M1, but another unknown cell was *shadow-filled*, presumably due to the transfer of dye from M1 at the level of the cell body or neurite. Neither the axon nor the dendrites of the shadow-filled cell could be identified. Fills of both M1 and M2 led to shadow-fills. None of the motor neurons with lateral cell bodies showed shadow-fills in the ventro-medial region of the SOG. Similar 'shadow-fills' were previously observed using a different fluorescent dye: rhodamine dextran (Schröter et al. 2007). The shadow-filled cell bodies were never associated with a complete neurite, nor was it ever possible to see the associated axon. From these observations, we deduced that the additional cell bodies were filled by dye that was transmitted from the recorded cell, presumably through channels in the cell bodies themselves. As these second cell bodies never filled sufficiently to see the associated dendrites, we were never able to determine which neuron had been co-filled. We presume that the medial neurons are connected through gap junctions on the somas that are sufficiently wide to transmit lucifer yellow and rhodamine dextran. We did not see multiple cell bodies when motor neurons with lateral cell bodies were filled.

long enough to record all possible physiological tests and to inject dye was difficult. Recording attempts were made from 157 animals. From these, we successfully recorded from and filled 30 neurons sufficiently to determine their identity.

We were able to record from and fill five identified neuron-types in the present study (M1, M2, L5, L7 and L8). We previously determined that the axon diameters of the other three cells were very small (<3 µm), which probably explains our inability to record and fill them (i.e. cells C3, L4 and L6). It was possible to use the morphologies of the cells to identify them between preparations. M1 and M2 are similar but M2 has a distinct bend in its neurite close to its dendritic arbours and it soon became evident that the two cells have different physiologies. Anatomically, L8 is easily distinguished from the other lateral cells because its cell body is located more lateral and anterior in the SOG. The only method for distinguishing the remaining lateral cells (L5 and L7) from each other involved dissection of the target muscle to determine which subunit was innervated by a given cell's terminals (Schröter et al. 2007). The difficulty of the latter procedure reduced the number of confirmed fills for L5 and L7. In total, we filled M1 on 10 occasions, M2 on 5 occasions, L5 on 4 occasions, L7 on 3 occasions and L8 on eight occasions.

Figure 2a shows a lucifer yellow fill of M1. The image shows the typically dense dendrites in the ipsilateral neuropile of the SOG. It also illustrates the very large size of the motor neuron cell body. An interesting feature of all the recorded cells was that a small dendrite always crossed into the dorsal region of the contralateral SOG. This image also shows a common finding when filling medial neurons. Fills of M1 and M2 always led to a second cell body being filled

General physiology

All the action potentials from the motor neurons in IK1 had the same characteristic properties: they tended to be broadly shaped and did not have large hyperpolarizations following the main depolarizing phase of the spike (Fig. 3). The MNs tended to have ongoing spontaneous activities but the actual spike rate could vary during recordings. On occasions, a neuron would temporarily become silent, with no spontaneous activity. After a few minutes, the spontaneous activity would suddenly return. This spontaneous firing rate is demonstrated for one cell (L8: Fig. 3a–c). The spiking activity was regular when present. After a sudden change in firing rate, the firing rate usually remained stable at the new rate for some time (usually several minutes). The recordings shown in Fig. 3a–c are from the same cell but at different times during the recording session. It is evident that in each case the firing rate is stable. The spontaneous firing rates can also be observed in the raster plots for other MNs (Figs. 4, 5). There were no obvious correlations between the sudden excursions from the regular firing pattern and external stimulation, and firing rates increased as often as they decreased suggesting a normal physiological mechanism rather than a deterioration of recording quality or damage to the cells. The sudden changes in spontaneous activity may reflect internal (locomotor) state changes, which have been recently reported to have an impact on the spontaneous activity in lobula plate tangential neurons in flies (Chiappe et al. 2010; Longden and Krapp 2009; Maimon et al. 2010). The response features outlined above were highly consistent between preparations suggesting real properties and not a problem with the recording technique. Exactly the same electrodes were also used to record from visually active descending neurons in the bee, as have been reported previously (Ibbotson and Goodman 1990).

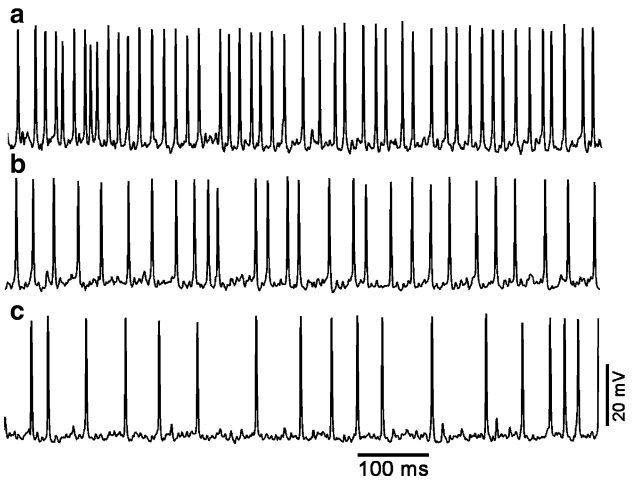

Fig. 3 Ongoing spontaneous spiking activity recorded from M1. The spikes in **a**, **b** and **c** were all recorded from the same cell at different times during the recording period. No stimulus was presented during any of the time periods shown. Spike rates tend to be fairly steady for long periods (minutes) but show transient shifts to new firing rates with no external stimulus. The action potentials are relatively broad compared to visual neurons earlier in the visual system. The action potentials are also monophasic (i.e. there is a single depolarization spike but no after-hyperpolarization)

Those recordings consistently revealed action potentials with narrower widths and clear hyperpolarising rebounds. It was also apparent that descending neurons generated higher spike frequencies than motor neurons.

For all cells, we qualitatively tested the sensitivity to air being blown over the head through a straw (by mouth) and to tapping the antennae with wooden tooth picks. All cells responded vigorously to these types of stimulation. Given the qualitative nature of the stimuli, we do not present these responses. It is clear that the cells receive input from mechano-sensory receptors and probably also from odour receptors (also see Menzel et al. 1991 for a recording from a motor neuron in a bee that had a cell body in the medial region of the SOG, similar to the cell in Fig. 2).

All of the recorded cells showed responses to visual stimulation. Responses consisted of clear fluctuations of the membrane potential. On most occasions, there were also changes in the action potential frequency. The mean membrane fluctuation of an M1 neuron in response to a flashed UV and green stimulus (stimulus device 2) is shown (Fig. 4a). There was a transient depolarization when the stimulus came on and a very brief hyperpolarization at the termination of the stimulus. The transient responses were due to a stimulus artefact that had zero delay created by the display (shown inset in Fig. 4a, marked: Stim. Art.). The artefact had no influence on the response of the neuron and was simply a pulse of electrical noise that we could not eliminate using shielding. It only occurred when the stimulus was turned ON or OFF, as clearly demonstrated by the inset figure. We did not subtract this from the response trace as we felt it important to present the raw data. The data show the total mean membrane fluctuation including any action potentials that were present. It is evident that a flashed stimulus (light ON, duration 200 ms) leads to a membrane depolarization. The artefact hyperpolarization is then followed by a depolarizing response to light OFF that persists for approximately 200 ms. Below the mean membrane potential, we show a raster plot of the action potentials (upper, Fig. 4b) and the spike density function from the same spike traces (lower, Fig. 4b). They demonstrate that the depolarizations are accompanied by an increase in spike rate both during light ON and after light OFF. The pattern of responses to flashed UV and green light is generally representative of responses from all the recorded cells, although the relative sizes of the ON and OFF responses varied between recordings within the same cell types and between cells. It appears that the cells carry information in their axons (which were the recording sites) both in the spike frequency and in slow fluctuations of the membrane potential and that the cells respond both to light ON and OFF.

As mentioned earlier, cells could suddenly (and apparently spontaneously) change their ongoing spiking rate. The recordings shown in Fig. 4a, b were obtained when the recorded cell had a prominent and regular ongoing firing rate (approximately 10 spikes/s). Several minutes later, this cell almost completely stopped producing spikes, yet it was clear that subthreshold responses to flashed stimuli were still present. In this changed state, the membrane potential showed the same general properties as had occurred during the previous stimulation, i.e. a depolarization during light ON, a brief hyperpolarization at light OFF and then a robust depolarization that persisted for 150 ms (Fig. 4c). However, throughout the trials only one spike was generated (upper, Fig. 4d). The data imply a very complex input network in which multiple inputs, perhaps some governed by internal state changes control the spiking behaviour.

Ocellar input

The honeybee has two visual systems, one receiving input from the compound eyes and the other from the three dorsally positioned simple eyes (ocelli) (Cajal 1918; Ribi 1975a, b; Goodman 1981). We wanted to determine whether both types of eyes (compound and ocelli) provided sensory input. It was not possible to only stimulate the ocelli using our system as stray light always fell on the compound eyes. However, it was possible to completely cover the ocelli with a black cap in such a way that no light fell upon them. We conducted experiments in which we tested the visual responses of the motor neurons with the

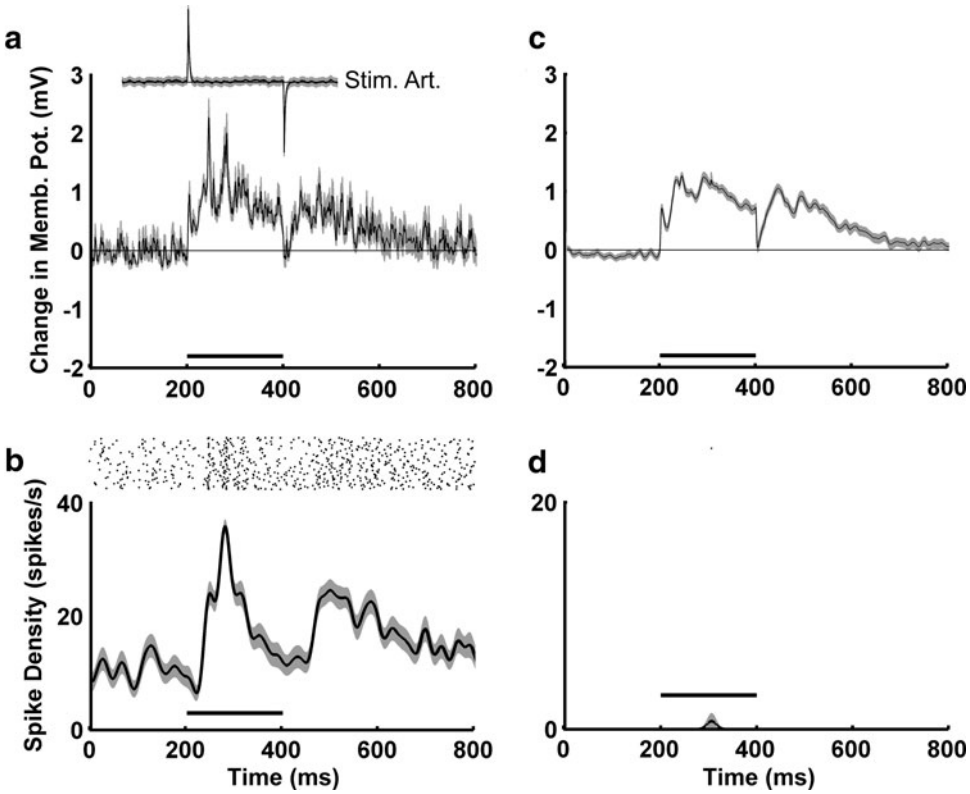

Fig. 4 Flash responses of M1. **a** Mean change in membrane potential during and after a 200 ms flash of combined UV and green light, using the LED-stimulus ($n = 55$). There is a short latency followed by a depolarization during the flash. After flash cessation, there is a transient hyperpolarization, then a prolonged depolarization. Shown inset (marked Stim. Art.) is a trace collected when the entire visual system was occluded from the stimulator but the stimulator was used as normal. It is clear that a stimulus artefact with zero latency, which could not be removed through grounding, was present. **c** Change in membrane potential for the same cell and the same stimulus, but in this case the cell had stopped spiking. The change in membrane potential appears smoother because there was only one spike included in the averages. The lower rows (**b**, **d**) show the spike arrival times (rasters) during 55 repetitions of the stimulus and the associated spike density functions. When the cell was in 'spiking mode' the pattern of spikes was similar (but slightly delayed) compared to the membrane fluctuations. Only one spike was produced during the stimulation shown in **d**. The *grey areas* show standard errors

ocelli covered (stimulus device 2). After results had been obtained, we removed the cap over the ocelli and repeated the experiments. Results were consistent between motor neurons, so a representative example is shown. Figure 5a shows the mean change in membrane potential during combined ocellar and compound eye stimulation for neuron M1. There is a clear depolarization during the 200 ms light-ON phase, followed by a hyperpolarization. These membrane changes are accompanied by a significant increase in spike rate during the stimulus (Fig. 5b). After the ocelli had been covered, there was a decrease in the amplitude of the membrane depolarization during the light-ON phase (Fig. 5c) and a dramatic difference in the spiking response (Fig. 5b). The spiking response showed virtually no excitation but, instead a suppression of the spontaneous activity. Very importantly, when the ocelli were covered, the spontaneous activity of the motor neuron increased from 30 spikes/s to nearly 50 spikes/s. This was a common observation in the motor neurons and strongly suggests that when the ocelli are illuminated by steady light they provide an ongoing suppressive signal to the motor neurons.

Visual motion responses

The responses to moving visual stimuli that we report were in most cases observed as increases in the ongoing spiking activity for certain selected directions of motion. Motion opposite to the preferred direction did not generally lead to significant inhibition of the spontaneous firing rate. Given that motion in this direction did not lead to inhibition, it is appropriate to use the term 'null direction'. The data presented in Fig. 6 show the general properties observed during motion stimulation in all cells. Brief movements of a black bar on a green background in the preferred direction generally led to a small membrane depolarization and an associated increase in spike rate (stimulus device 2, right hand traces, Fig. 6a). When the bar moved in the null

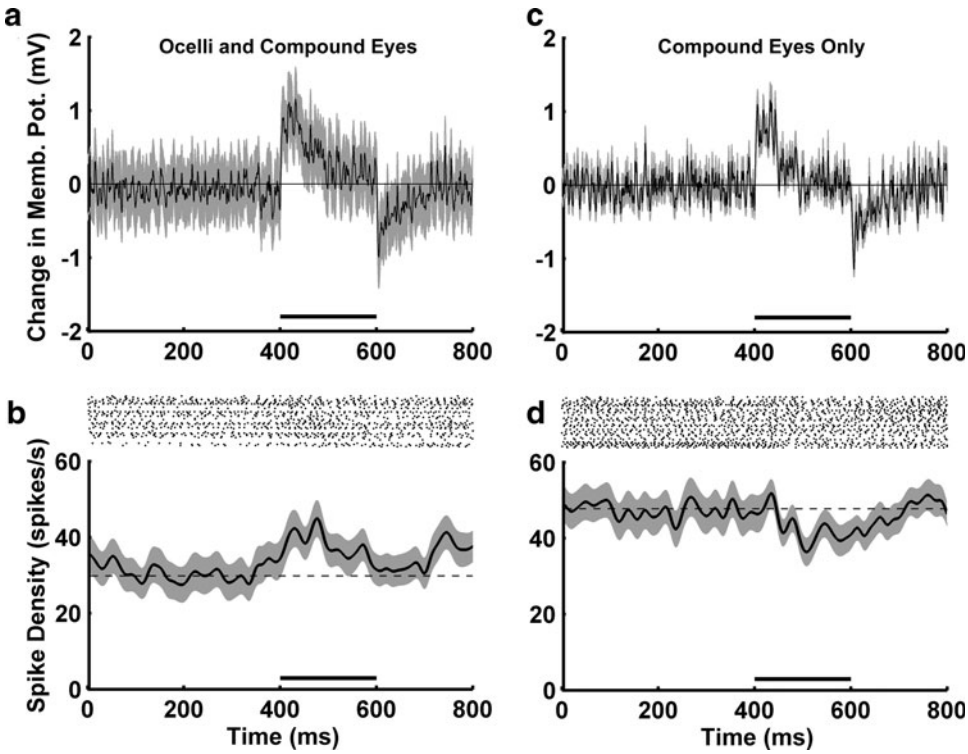

Fig. 5 Flash responses of M1, with and without the presence of the ocelli. **a**, **c** Mean change in membrane potential during and after a 200 ms flashed light stimulus (UV and Green) with either **a** combined ocellar and compound eye, or **c** compound eye only stimulation ($n = 45$). There is a clear depolarization during the 200 ms light-ON phase. The lower rows (**b**, **d**) show the spike arrival times (rasters) during 45 repetitions of the stimulus and the associated spike density functions. **b** With combined ocellar and compound eye stimulation, there is a small but significant increase in spike rate during the stimulus compared to the compound eye-only condition. **d** The spiking response shows a suppression of spontaneous activity with only compound eye stimulation. The *grey areas* show standard errors

direction there was no variation in either the membrane potential or the spike frequency (left hand traces, Fig. 6a).

Throughout the rest of the paper, we present quantitative data based on spike frequencies when the bees were stimulated using moving gratings presented on a visual monitor (stimulus device 1). Care was taken to measure the entire directional and temporal tuning during a period of stable spontaneous activity. The data in Fig. 6b show responses to 3 s periods of grating motion in eight different directions for an identified L8 neuron that had its axon on the right hand side of the animal. As was usually the case, the cell had a robust ongoing activity. Motion to the right (progressive motion over the eye) generated a significant increase in firing rate (t test, $P < 0.01$), while motion to the left showed no significant change in firing rate compared to controls (t test, $P > 0.05$). In the example shown, motion downward and to the right (45° down) also led to a significant increase in firing rate (t test, $P < 0.01$). There was no significant change in firing rate relative to the mean ongoing rate for the other directions.

Directional and temporal tuning of neurons innervating muscle 51

The following convention is used when describing directional tuning. All descriptions are for cells in the left hand side of the body. Rightward motion equates to 0°, upward motion 90°, leftward motion 180° and downward motion 270°. Therefore, 180° is progressive motion over the left eye (i.e. motion from right to left and from front to back).

L8

From the eight L8 neurons, we identified anatomically, the directional tuning was measured in full on six occasions. The cell has a lateral cell body and a distinctive long neurite, which makes identification relatively easy (Fig. 7a; Schröter et al. 2007). The ongoing spike rates ranged from 0 to 28 spikes/s between cells (e.g. Fig. 7). The directional preferences were always for progressive motion over the ipsilateral eye, e.g. leftward motion for a cell with its axon on the left hand side of the nervous system (Fig. 7b). The tuning functions were broad: the stars in Fig. 7b show directions of motion that led to significant increases in spiking rate for one cell (t test, $P < 0.01$). The mean preferred direction for the six neurons was 187° ± 3.0SE ($n = 6$). Stimulation of the contralateral eye with the ipsilateral eye covered produced only very small visual responses. This cell type was maximally sensitive to high TFs, with optima at 8–24 Hz (Fig. 7c). The mean TF optimum was 13.3 Hz ± 4.6 SE ($n = 6$).

M2

While M2 was filled on five occasions in total, we only determined directional tuning in three preparations. It has a ventro-medial cell body location, a distinct kink in its

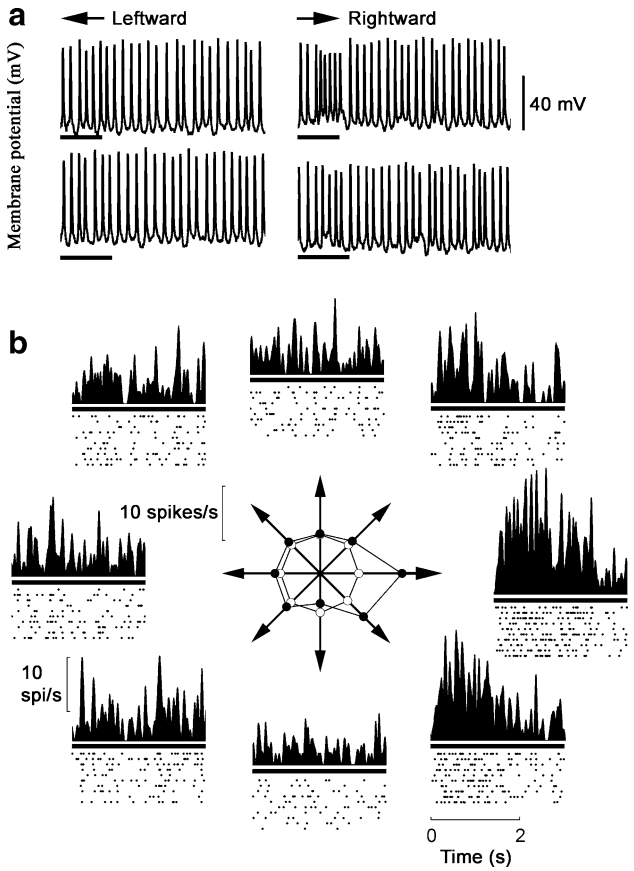

Fig. 6 Motion responses. **a** Spike trains during and after the movement of a vertical green bar that was moved horizontally across the receptive field of L8 to the left (*left hand traces*) and then to the right (*right hand traces*). The *bar* was moved at two speeds (upper, 100°/s; lower, 200°/s). The L8 neuron was on the right hand side of the nervous system. Motion to the right generates an increase in spike rate and a small depolarization of the membrane potential. Motion to the left does not influence the membrane potential or the spike rate. **b** Responses from another L8 neuron, again recorded on the right hand side of the nervous system. Responses to 3 s of wide-field grating motion are shown for 8 directions of motion. Both rasters and spike density functions are shown. The *inner arrows* show the directions of motion and the mean firing rates for each direction of motion (*solid symbols*). The mean spontaneous rate for this cell during these recordings was 10.2 spikes/s (*open symbols*). Significant increases in firing rate were obtained from this cell to rightward and rightward-down motion

neurite and largely confines its dendrites to the upper regions of the SOG. Its morphology is characteristically different to M1, thus making it possible to identify it with relative ease (Fig. 7d). Spontaneous rates were 6–35 spikes/s in the recorded cells. The cells consistently preferred progressive image motion over the ipsilateral eye, although the directions of motion that produced increased spike rates were broad (Fig. 7e). The stars in Fig. 7e show directions of motion that led to significant increases in spiking rate for one cell (*t* test, $p < 0.01$). The mean preferred direction for the three neurons was 183° ± 6.7SE ($n = 3$). Stimulation of the contralateral eye (ipsilateral eye covered) produced only small responses, suggesting that the cell receives mainly ipsilateral eye input. The temporal frequency (TF) tuning showed a preference for high TFs, with a mean peak value of 32 Hz ± 16.0SE ($n = 3$) (Fig. 7f).

Directional and temporal tuning of neurons innervating muscle 44

L5

Four confirmed recordings were obtained from this cell type but directional tuning was determined in only two preparations (Fig. 8a). The terminals were located in the dorsal-B subunit of muscle 44, which is what allowed unique identification (Schröter et al. 2007). The spontaneous activities in all cases were high (20–85 spikes/s). There was variation in the ongoing spike rate during each recording but it was relatively minor (30% over time). The directional tuning was consistent, with both cells showing a preference for regressive image motion when the stimulus was positioned frontally (Fig. 8b). The average preferred direction for the two cells was 351° ($n = 2$). Clear responses were observed when the ipsilateral and contralateral eyes were stimulated by regressive motion. The TF tuning was also consistent, with peak TF tuning of 8 and 16 Hz in the two cells examined in full (Fig. 8c).

L7

Confirmed recordings were made from this cell type on three occasions (Fig. 8d). The terminals were located in the medial subunit of muscle 44 (Schröter et al. 2007). The spontaneous activities were 0–30 spikes/s between preparations and were highly consistent for individual cells (variation of 10–20% during recordings). The directional tuning of all recorded cells showed high consistency, with all cells preferring regressive motion during frontal stimulation (Fig. 8e). The mean preferred direction was 348° ± 3.5°SE ($n = 3$). A clear characteristic of this cell class was a preference for lower TFs (Fig. 8f). The maximum response was recorded for a TF of 3 Hz ± 1.7 SE ($n = 3$), while at 24 Hz the cell hardly responded.

M1

Successful recordings and fills from M1 were confirmed in 10 preparations. We were able to determine the directional tuning in six of these preparations. A photograph of one fill is presented in Fig. 2 and a drawing of another fill (Fig. 9a). The cell has three characteristic sweeping dendrites that descend from the dorsal to the ventral SOG. This characteristic, combined with the ventral cell body make identification between preparations particularly easy. M1 had a high

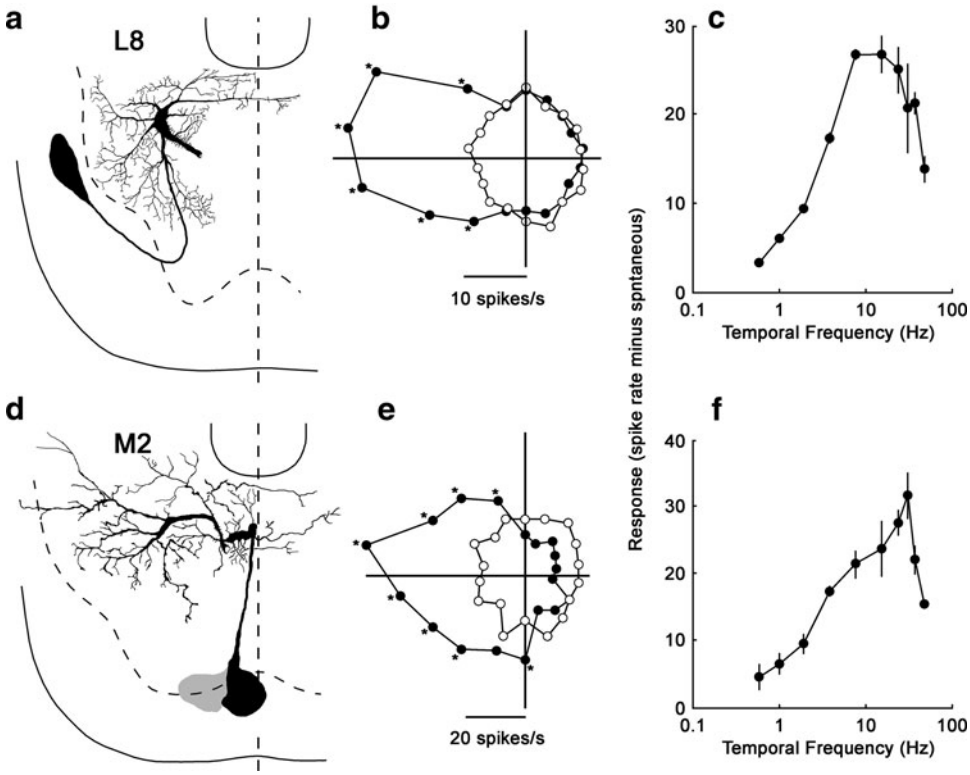

Fig. 7 **a** A sketch of an L8 neuron in the SOG. Its directional and temporal frequency tuning are shown in **b**, **c**. **d** Sketch of a recorded M2 neuron, along with its directional and temporal tuning (**e**, **f**). Both cells respond maximally to progressive motion at high temporal frequencies of (8–24 Hz). *Error bars* represent standard errors

spontaneous activity in all recordings, which ranged from 0 to 94 spikes/s. The spontaneous activity fluctuated by as much as 400% from the lowest measured spontaneous rate for prolonged periods during the recording. The fluctuations in spontaneous rate were not always correlated with stimulus manipulations. The cell produced robust responses when presented with full field flashing stimuli and gave weak directional responses when tested with wide-field motion (Fig. 9b). The mean directional tuning was 357° ± 5.2°SE ($n = 6$). The cell responded to stimulation of both eyes. A range of temporal frequencies of motion was tested and responses were most robust at high values (16–32 Hz, Fig. 9c). The mean TF optimum was 16 Hz ± 6.5°SE ($n = 4$).

Discussion

Our study has for the first time identified the specific directional tuning characteristics of five uniquely identifiable motor neurons in the honeybee. These neurons innervate two of the muscles found on each side of the body in the neck region. The study revealed that each cell was optimally tuned to detect horizontal image motion at high temporal frequencies. The cells were found to receive input from both visual systems in the bee, the compound eyes and the ocelli. Moreover, all the cells were observed to respond to air currents and tactile stimulation of the head and antennae. Based on this data, we now discuss the relation between the directional tuning of the cells and the potential role of the neurons in driving head movements.

General characteristics

While the main focus of the present study was to investigate visual responses, it is clear that the motor neurons are multisensory, as is the case for fly neck motor neurons (Milde et al. 1987). While our air stimulation technique was not quantitative, it clearly revealed robust responses when air was blown over the heads of the animals. Cells in the bee that anatomically resemble M1 and M2 have been shown to respond to olfactory stimulation, and to have learning capacity (Menzel et al. 1991). Huston and Krapp (2008) have suggested that neck motor neurons in the fly are tuned to activate neck muscles during specific optic flow patterns, which are induced by particular types of self-motion. We did not measure the specific optic flow sensitivities of the motor neurons in the bee but certainly, we have found that all five recorded neuron types are sensitive to motion in the horizontal plane, suggesting a role in head yaw stabilization. It is highly likely that the air currents generated by such movements are detected by sensory hairs and that this information is combined with visual input to provide selective stimulation of the neck motor neurons during flight. Descending neurons that connect the brain

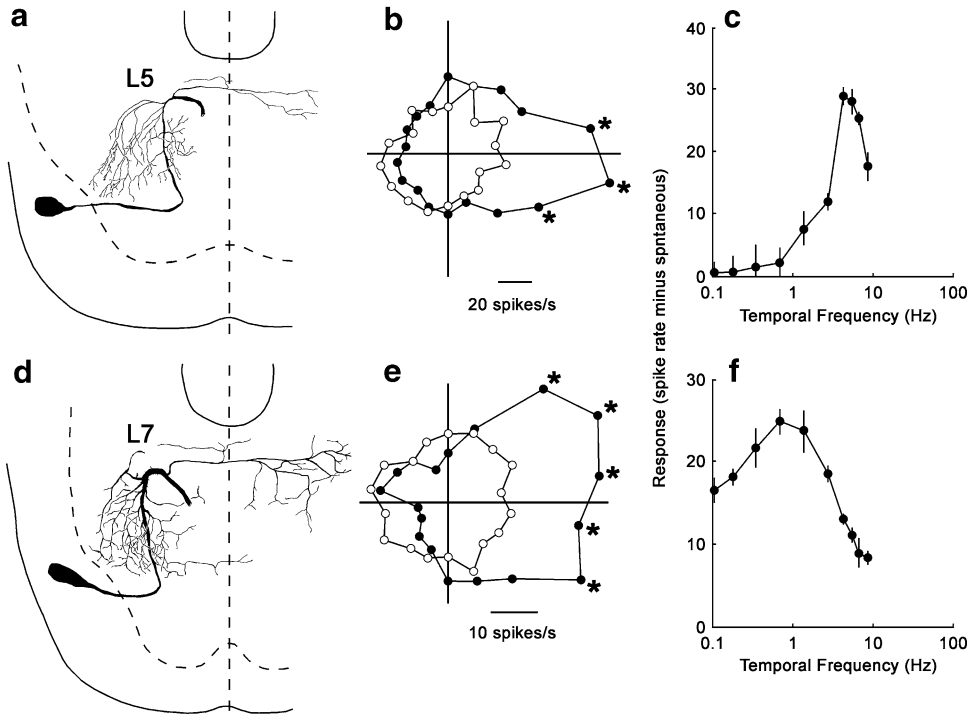

Fig. 8 **a** A sketch of an L5 neuron in the SOG. Its directional and temporal frequency tuning are shown in **b**, **c**. **d** Sketch of a recorded L7 neuron, along with its directional and temporal tuning (**e**, **f**). Both cells respond to regressive motion. L5 responds optimally at high temporal frequencies (5–10 Hz), while L7 responds at lower temporal frequencies (1 Hz). *Error bars* represent standard errors

and thoracic motor centres in the locust have been shown to accurately coordinate visual and tactile senses to generate turning responses (Reichert et al. 1985; Reichert and Rowell 1986).

The bee, like most insects has two types of eyes, the compound eyes and the simple eyes (ocelli) (shown schematically in Fig. 10). With the ocelli covered visual responses changed and spontaneous activities increased. It is plausible that stimulation of the ocelli needs to roughly match particular rotation axes before sensor fusion between the two visual systems occurs (Parsons et al. 2010). Even if this is the case, we have shown that there is a clear sensory input from both the ocelli and the compound eyes. It is intriguing that with the ocelli uncovered the spontaneous rates went down, suggesting that the ocelli provide a generalised suppression of the ongoing activity when they were exposed to the ambient light conditions in the laboratory. Honeybee ocellar neurons are excited by light off and suppressed by light on (Milde 1981). It appears that ongoing light levels directed at the ocelli drive suppressive signals that reduce the ongoing spiking activities of downstream neurons, including neck motor neurons.

The motor neurons were not disconnected from the muscles and, while the head and prothorax were firmly secured to the thorax with wax, the muscles within the prothorax were able to contract and relax at any time. We presume that the steady firing rates observed during non-stimulation periods (Fig. 3) are most likely position signals that drive a particular muscle contraction state. Under natural conditions, this would equate to a particular head position relative to the thorax. The sudden non-stimulus related changes in spiking rates probably signal an internally generated command to change head position. The stability of the ongoing signals resembles the position signals, for example observed in the abducens motor neurons of the primate (Fuchs and Luschei 1970), which drive eye movements for many of the same reasons as the muscles of the bee drive head movements (e.g. to stabilize retinal images). We presume that the sudden increase in the frequency of action potentials generated by our visual stimuli would be sufficient to drive a change in muscle and, therefore, head position and speed. Gilbert et al. (1995) have shown that electrical stimulation of selected neck muscles in flies leads to movements of the head.

Directional tuning

Two cells innervate muscle 51 (M2 and L8: Schröter et al. 2007). M2 innervates the dorsal subunit of the muscle and L8 innervates the ventral subunit. Both muscle subunits connect the rear of the prothoracic cavity (the endosternum) with the cervical apodeme of the episternum (CAE), which is located at the anterior end of the prothoracic cavity (Fig. 1a, b; Snodgrass 1942; Schröter et al. 2007). Muscle 51 is aligned such that it pulls the CAE inwards towards the centre of the prothorax (Fig. 10). Head turning in bees is a complex process, as recently revealed through three-dimensional modelling of the head–neck system (Berry and Ibbotson 2010). There are only five pairs of muscles that

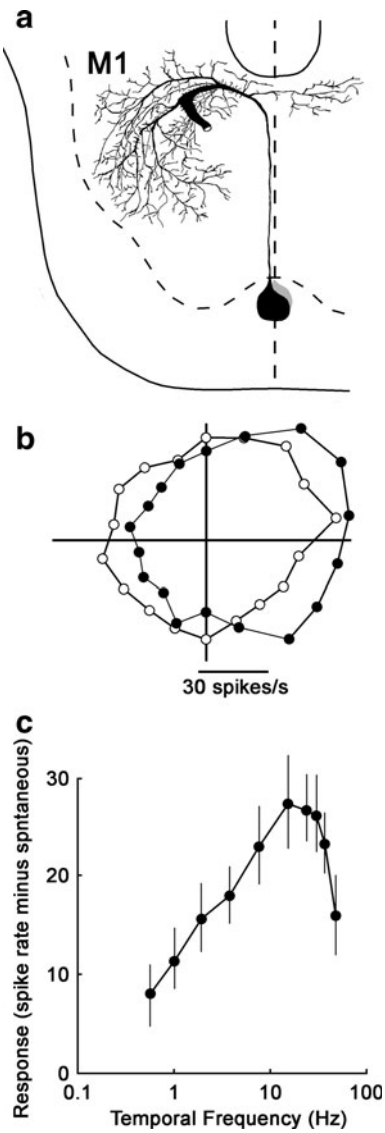

Fig. 9 **a** A sketch of an M1 neuron in the SOG. Its directional and temporal frequency tuning are shown in **b**, **c**. M1 was optimally sensitive to high temporal frequencies of motion (>16 Hz). *Error bars* represent standard errors

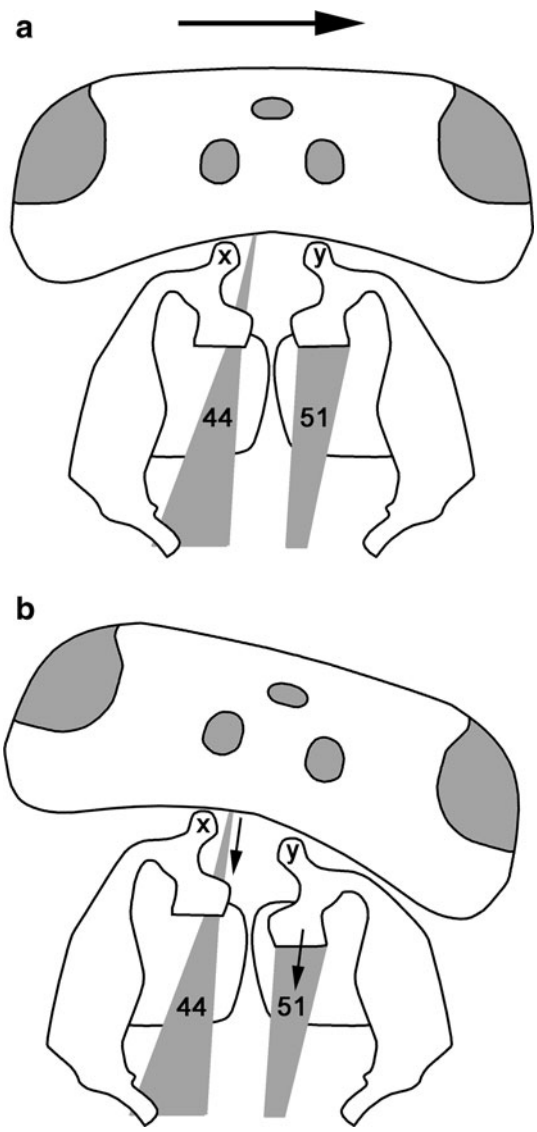

Fig. 10 Organisation of yawing head turns in bees. **a** The head and prothorax with the head in the normal position, as viewed from above. *x* and *y* are the occipital processes and the numbered grey structures are the muscles 44 and 51 that would be involved in a rightward head turn. On the head, we have outlined in grey the dorsal regions of the compound eyes and the three ocelli. During image motion to the right (*black arrow*), optomotor head turning occurs, which drives the head to the right, as shown in **b**. To make the head turn to the right muscle 51 contracts, thus pulling the point *y* inwards. Other direct muscles, including muscle 44 also contract, thus turning the head to the right using point *x* as the fulcrum

connect the prothorax with the head. These muscles are able to drive head inclination (nose-up pitch) and declination (nose-down pitch) without involvement from other muscles in the thorax. However, head yaw and roll require far more complex interplay between the direct muscles and 12 pairs of indirect muscles that rotate the prothorax relative to the thorax or deform the shape of the prothoracic exoskeleton. The most likely role for the direct muscles during head yaw and roll is to retract the head firmly towards the prothorax (see small arrow close to the head of muscle 44 in Fig. 10b). This retraction effectively fixes the head to the prothorax. The 12 pairs of indirect muscles can rotate the prothorax within the thoracic cavity and, because the head is secured to it, also move the head relative to the thorax. For yaw, the head cannot rotate in the horizontal plane because it rests on two horizontally aligned pivot points (the occipital processes). These are indicated in Fig. 10 as '*x*' and '*y*'. For the head to yaw, it is necessary for the occipital processes to be differentially retracted. That is, to turn the head to the right, the right hand occipital process (*y*) needs to be pulled inwards towards the prothorax (as is the case in Fig. 10b). This action 'makes space' for the head so that it can tilt to the right using the left

occipital process (*x*) as the fulcrum. It is probable that the contracting direct muscles force the head to move into that space. It is muscle 51 that has the most significant effect on retracting the occipital process (Fig. 1a, b). During dissection, we attempted to retract the CAE and found that the exoskeleton at the base of the CAE is highly flexible (Berry and Ibbotson 2010).

Both M2 and L8 respond maximally to progressive image motion (motion towards the side containing the innervated muscle). When the image moves progressively, both MNs will respond optimally and provide maximum drive to muscle 51. This activity presumably leads to a muscle contraction, which pulls the ipsilateral occipital process inwards, thus in concert with other muscles turning the head towards that side of the body. A head turn in the direction of image motion acts to stabilize the retinal image and is referred to as an optomotor head turning response (van Hateren and Schilistra 1999). In conclusion, the directional tuning of both M2 and L8 are well suited to a role in driving progressive optomotor head turning in the bee in response to progressive image motion across the retina.

The control of muscle 44 is considerably more complex. This muscle is innervated by six neurons, of which we were able to record from three. All three neurons had consistent directional tuning properties: they all responded optimally to regressive image motion, as did the unit-type 2 reported using extracellular recording (Schröter et al. 2007). In itself, this finding is a surprise because muscle 44 appears to be arranged to activate head declination (nose-down pitch). To find that the cells innervating the muscle have horizontal tuning suggests a far more complex role for the muscle.

The directional tuning makes it possible that muscle 44 is involved in the control of yawing head movements. One role is probably to act with other direct muscles to anchor the head to the prothorax during head yaw. That is, when a horizontal head turn is about to occur, muscle 44 is contracted to retract the head towards the thorax. Muscle 44 connects centrally, medial to the occipital processes (Fig. 10b). Thus, even activation of this muscle on the left side of the nervous system will assist in turning the head to the right if simultaneous deformation of the right hand CAE (via the right hand muscle 51) has made a space for the head to move into. It is presumed that other direct muscles on the ipsilateral side of the body (right hand side in Fig. 10) also contract to drive yawing head movements (Berry and Ibbotson 2010).

Temporal frequency tuning

Of the five cell types reported here, four were optimally activated by high temporal frequencies in the range from 8 to 32 Hz. It is interesting to correlate the temporal frequency properties to those of the descending neurons that potentially provide the visual input to the motor neurons. Recordings from descending neurons in the bee have revealed several identifiable neurons sensitive to motion in the same directions as those reported for the motor neurons presented here (Ibbotson and Goodman 1990; Ibbotson 1991). While no actual connectivity between the descending neurons and the motor neurons has been shown, the collaterals of the former clearly intermingle with the dendrites of the MNs in the suboesophageal ganglion. The temporal tuning of these horizontally tuned descending neurons is very similar to that of the MNs, with peaks in the range from 8 to 20 Hz (Ibbotson and Goodman 1990). Direction-selective neurons in the lobula of the bee, which presumably provide input to the descending neurons described above, also exhibit very similar directional and temporal tuning to the motor neurons in IK1 (Ibbotson 1991; O'Carroll et al. 1996). Thus, the potential pathway from lobula to descending neurons to motor neurons in the bee reveals a consistency of temporal tuning. The temporal frequency dependence of optomotor head turning reflexes have not been measured in bees, however, the frequency tuning of optomotor body turning responses have been reported (Kunze 1961). That study revealed a peak temporal frequency tuning of 10 Hz, which again reasonably matches the data from the motor neurons in IK1.

For all the motor neurons reported here, low spatial frequency gratings produced the largest responses, as shown previously with extracellular recordings from IK1 (Schröter et al. 2007). We used a spatial frequency of 0.02 cpd for virtually all experiments. Thus, given that speed is the ratio of temporal and spatial frequency, the optimal speed tuning for the cells was very high (400–1,600°/s). Based on observations of bees in flight, it appears that they attempt to maintain optic flow speeds of between 200 and 600°/s (Baird et al. 2005; Srinivasan et al. 1996). These speeds were based on the movement of the bee itself and it can be assumed that even more rapid image speeds would be generated when the bee moves its head during flight. In the fly, it has been shown that head turns during normal flight can be very fast (hundreds or thousands of degrees per second: van Hateren and Schilistra 1999). The optimum optic flow speed sensitivities observed in the motor neurons of the bee neck appear to be appropriate for the behavioural environment in which bees operate.

One cell type (L5) had consistently lower temporal frequency optima (4 Hz). This equates to 200°/s given a spatial frequency of 0.02 cpd, which is lower but not particularly slow. It would appear that some type of speed-related range fractionation exists within the bee motor control system. It has been suggested that it is useful to have cells tuned to lower speeds for behaviours such as hovering

close to flowers or scanning outside the nest in certain insect species, including bees (O'Carroll et al. 1996). Certainly, it is typical for direction-selective visual neurons in birds and mammals to have a range of speed tuning properties within a given species (Ibbotson and Price 2001; Ibbotson and Mark 1996).

Acknowledgments To our knowledge, the first people to record from neurons in IK1 were Christopher J. Pomfrett and Lesley J. Goodman (unpublished observations). This preliminary work motivated the present study. The LED-based visual stimulator was developed by Dr Gert Stange. Dr Richard Berry developed the three-dimensional model of the bee neck used to generate Fig. 1a, b.

References

Baader A (1991) The contribution of some neck and abdominal motoneurones in locust (*Locusta migratoria*) steering reactions. J Insect Physiol 37:689–697

Baird E, Srinivasan MV, Zhang S, Cowling A (2005) Visual control of flight speed in honeybees. J Exp Biol 208:3895–3905

Batschelet E (1981) Circular statistics in biology. Academic Press, London

Berry R, Ibbotson M (2010) A three-dimensional atlas of the honeybee neck. PLoS ONE 5(5):1–14

Berry R, Stange G, Olberg R, van Kleef J (2006) The mapping of visual space by identified large second-order neurons in the dragonfly median ocellus. J Comp Physiol A 192:1105–1123

Böddeker N, Hemmi JM (2010) Visual gaze control during peering flight manoeuvres in honeybees. Proc R Soc B Biol Sci 277:1209–1217

Böddeker N, Dittmar L, Stuerzl W, Egelhaaf M (2010) The fine structure of honeybee head and body yaw movements in a homing task. Proc R Soc B Biol Sci 277:1899–1906

Cajal SR (1918) Observaciones sobre la estructura de los ocelos y vias nerviosas ocelars de algunos insectos. Trab Lab Invest Biol Ubiv Madrid 16:109–139

Chiappe M, Eugenia SJD, Reiser MB, Jayaraman V (2010) Walking modulates speed sensitivity in Drosophila motion vision. Curr Biol 20:1470–1475

Fuchs AF, Luschei ES (1970) Firing patterns of abducens neurons of alert monkeys in relationship to horizontal eye movement. J Neurophysiol 33:382–390

Gilbert C, Gronenberg W, Strausfeld NJ (1995) Oculomotor control in calliphorid flies - head movements during activation and inhibition of neck motor-neurons corroborate neuroanatomical predictions. J Comp Neurol 361:285–297

Goodman LJ (1981) Organisation and physiology of the insect dorsal ocellar system. In: Autrum H (ed) Handbook of sensory physiology, vol VII/6C. Springer, Berlin, pp 201–286

Hausen K (1982) Motion sensitive interneurons in the optomotor system of the fly.2. The horizontal cells—receptive-field organization and response characteristics. Biological Cybernetics 46:67–79

Hengstenberg R (1984) Roll-stabilization during flight of the blowfly's head and body by mechanical and visual cues. In: Varju D, Schnitzler U (eds) Localization and orientation in biology and engineering. Springer, Berlin, pp 121–134

Hengstenberg R, Sandeman DC, Hengstenberg B (1986) Compensatory head roll in the blow fly Calliphora during flight. Proc R Soc Lond B 227:455–482

Huston SJ, Krapp HG (2008) Visuomotor transformation in the fly gaze stabilization system. PLOS Biol 6:1468–1478

Huston SJ, Krapp HG (2009) Nonlinear integration of visual and haltere inputs in fly neck motor neurons. J Neurosci 29:13097–13105

Ibbotson MR (1991) A motion-sensitive visual descending neurone in *Apis mellifera* monitoring translatory flow-fields in the horizontal plane. J Exp Biol 157:573–577

Ibbotson MR, Crowder NA, Cloherty SL, Price NSC, Mustari MJ (2008) Saccadic modulation of neural responses: possible roles in saccadic suppression, enhancement and time compression. J Neurosci 28:10952–10960

Ibbotson MR, Goodman LJ (1990) Response characteristics of four wide-field motion-sensitive descending interneurons in *Apis mellifera*. J Exp Biol 148:255–279

Ibbotson MR, Mark RF (1996) Impulse responses distinguish two classes of directional motion-sensitive neurons in the nucleus of the optic tract. J Neurophysiol 75:996–1007

Ibbotson MR, Price NSC (2001) Spatiotemporal tuning of directional neurons in mammalian and avian pretectum: a comparison of physiological properties. J Neurophysiol 86:2621–2624

Ibbotson MR, Price NSC, Crowder NA, Ono S, Mustari MJ (2007) Enhanced motion sensitivity follows saccadic suppression in the superior temporal sulcus of the macaque cortex. Cereb Cortex 17:1129–1138

Karmeier K, van Hateren JH, Kern R, Egelhaaf M (2006) Encoding of naturalistic optic flow by a population of blowfly motion-sensitive neurons. J Neurophysiol 96:1602–1614

Kern R, van Hateren JH, Michaelis C, Lindemann JP, Egelhaaf M (2005) Function of a fly motion-sensitive neuron matches eye movements during free flight. Plos Biol 3:1130–1138

Krapp HG, Hengstenberg R (1996) Estimation of self-motion by optic flow processing in single visual interneurons. Nature 384:463–466

Kunze P (1961) Untersuchung des bewegungssehens fixiert fliegender bienen. Zeitschrift fur Vergleichende Physiologie 44:656–684

Land MF (1973) Head movements of flies during visually guided flight. Nature 243:299–300

Lindemann JP, Kern R, Michaelis C, Meyer P, van Hateren JH, Egelhaaf M (2003) Flimax, a novel stimulus device for panoramic and highspeed presentation of behaviourally generated optic flow. Vis Res 43:779–791

Lindemann JP, Weiss H, Moeller R, Egelhaaf M (2008) Saccadoc flight strategy facilitates collision avoidance: closed-loop performance of a cyberfly. Biol Cybern 98:213–227

Longden K, Krapp H (2009) State-dependent performance of optic flow processing interneurons. J Neurophysiol 102:3606–3618

Maimon G, Straw AD, Dickinson MH (2010) Active flight increases the gain of visual motion processing in Drosophila. Nat Neurosci 13:U29–U393

Markl H (1966) Peripheres Nervensystem und Muskulatur im Thorax der Arbeiterin von *Apis mellifica* L., *Formica polyctena* Foerster und *Vespa vulgaris* L. und der Grundplan der Innervierung des Insektenthorax. Zool Jb Anat 83:107–184

Menzel R, Hammer M, Braun G, Mauelshagen J, Sugawa M (1991) Neurobiology of learning and memory in honeybees. In: Goodman L, Fisher R (eds) The behaviour and physiology of bees. CAB International, Wallingford, pp 323–353

Milde J (1981) Graded potentials and action potentials in the large ocellar interneurons of the bee. J Comp Physiol A 143:427–434

Milde J, Seyan H, Strausfeld NJ (1987) The neck motor system of the fly *Calliphora erythrocephala* II. Sensory organization. J Comp Physiol A 160:225–238

O'Carroll DC, Bidwell NJ, Laughlin SB, Warrant E (1996) Insect motion detectors matched to visual ecology. Nature 382:63–66

Parsons MM, Krapp HG, Laughlin SB (2010) Sensor fusion in identified visual interneurons. Curr Biol 20:624–628

Reichert H, Rowell CHF, Griss C (1985) Course correction circuitry translates feature detection into behavioural action in locusts. Nature 315:142–144

Reichert H, Rowell CHF (1986) Neuronal circuits controlling flight in the locust: how sensory information is processed for motor control. TINs 9:281–283

Ribi WA (1975a) The first optic ganglion of the bee. I. Correlation between visual cell types and their terminals in the lamina and medulla. Cell Tissue Res 165:103–111

Ribi WA (1975b) The neurons in the first optic ganglion of the bee (*Apis mellifera*). Adv Anat Embryol Cell Biol 50:1–43

Schröter U, Wilson S, Srinivasan MV, Ibbotson MR (2007) The morphology and physiology of suboesophageal neck motoneurons in the honeybee. J Comp Physiol A 193:289–304

Snodgrass RE (1942) The skeleto-muscular mechanisms of the honey bee. Smithson Misc Collect 103:1–120

Sobel EC (1990) The locust's use of motion parallax to measure distance. J Comp Physiol 167:579–588

Srinivasan M, Zhang S, Lehrer M, Collett T (1996) Honeybee navigation en route to the goal: visual flight control and odometry. J Exp Biol 199:237–244

Strausfeld NJ, Seyan H, Milde JJ (1987) The neck motor system of the fly *Calliphora erythrocephala* I. Muscles and motor neurons. J Comp Physiol A 160:205–224

van Hateren JH, Schilstra C (1999) Blowfly flight and optic flow II. Head movements during flight. J Exp Biol 202:1491–1500

Wertz A, Gaub B, Plett J, Haag J, Borst A (2009a) Robust coding of ego-motion in descending neurons of the fly. J Neurosci 29:14993–15000

Wertz A, Haag J, Borst A (2009b) Local and global motion preferences in descending neurons of the fly. J Comp Physiol 195:1107–1120